Available online at www.sciencedirect.com
SCIENCE DIRECT®
ELSEVIER
Journal of Computational and Applied Mathematics 173 (2005) 1–19
JOURNAL OF COMPUTATIONAL AND APPLIED MATHEMATICS
www.elsevier.com/locate/cam

Reduced-order-based feedback control of the Kuramoto–Sivashinsky equation

C.H. Lee[a,*], H.T. Tran[b]

[a] *Department of Mathematics, California State University, Fullerton, CA 92834-6850, USA*
[b] *Center for Research in Scientific Computation, North Carolina State University, Raleigh, NC 27695-8205, USA*

Received 13 February 2002; received in revised form 14 January 2004

Abstract

In this paper, we consider the Kuramoto–Sivashinsky equation (KSE), which describes the long-wave motions of a thin film over a vertical plane. Solution procedures for the KSE often yield a large or infinite-dimensional nonlinear system. We first discuss two reduced-order methods, the approximate inertial manifold and the proper orthogonal decomposition, and show that these methods can be used to obtain a reduced-order system that can accurately describe the dynamics of the KSE. Moreover, from this resulting reduced-order system, the feedback controller can readily be designed and synthesized. For our control techniques, we use the linear and nonlinear quadratic regulator methods, which are the first- and second-order approximated solutions of the Hamilton–Jacobi–Bellman equation, respectively. Numerical simulations comparing the performance of the reduced-order-based linear and nonlinear controllers are presented.

Keywords: Viscous film flows; Kuramoto–Sivashinsky equation; Nonlinear feedback control; Approximate inertial manifold; Proper orthogonal decomposition

1. Introduction

The problem of influencing a fluid flow to behave in a desirable fashion has been studied by numerous scientists over the centuries. Due to the complexity of the dynamics of fluid, the nature of the application, and the cost of building experimental laboratories, most studies have been conducted using computer simulation. Even with today's computational capabilities, numerical calculations and control of many fluid dynamic problems are still considered *impracticable*. The main challenge lies in the continuous description of the fluid flow, which requires solving a very large system of ordinary

* Corresponding author.
E-mail addresses: hlee@newton.fullerton.edu (C.H. Lee), tran@control.math.ncsu.edu (H.T. Tran).

0377-0427/$ - see front matter © 2004 Published by Elsevier B.V.
doi:10.1016/j.cam.2004.02.021

differential equations. As a result, the controller is complicated and is of high dimension. The purpose of this study is to overcome such difficulty by taking advantage of the reduced-order techniques, called the *approximate inertial manifold* (AIM) and the *proper orthogonal decomposition* (POD) methods. Namely, we develop a technique that systematically replaces a large complicated physical system by another system, which is simpler, smaller, and equivalent. The most important consequence of this in our work is that the reduced order system is small enough to use so that one can generate a real-time on-line feedback control, whereas the system resulting from a generic discretization (e.g., a standard finite difference or finite element method) would require too much time to solve, hence, rendering it inapplicable in real-time control applications.

The AIM method is based on the theory of inertial manifolds for dissipated evolutionary partial differential equations and has been applied to a number of important equations in fluid dynamics and mathematical physics [13–15,17,18,20,21,46,51]. Due to the dissipativity, all solution trajectories in the phase space are attracted to the global attractor, which may be complicated or even fractal. An inertial manifold for a dissipative system is, on the other hand, a finite dimensional Lipschitz manifold, which is positively invariant under the solution evolution, and which attracts all bounded sets in the phase space. As a result it necessarily contains the global attractor. The solution flow restricted to an inertial manifold is equivalent to that of a finite dimensional system of ordinary differential equations called an *inertial form*. Numerical procedures to solve the inertial form are known as the AIM methods or the *nonlinear Galerkin* methods, which have been employed in solving a number of important equations in fluid dynamics and mathematical physics, such as the Navier–Stokes equations [28,29,53], Burgers equation [38], reaction diffusion equations [39], the Cahn–Hilliard equation [40], and the Kuramoto–Sivashinsky equation [27,52].

The POD method has received much attention in recent years as a tool to analyze complex physical systems. In principle, the idea is to use laboratory equipment to make measurements or to use a reliable solver to compute a priori an ensemble of solutions to a physical model. These measurements or solutions are called *snapshots*. Applying the POD technique to these snapshots produces an "optimal" representation, in the sense that, it uses the least degrees of freedom to represent the ensemble. This process is also known as the *Karhunan Loève* procedure or *principle component analysis*. When the POD method is applied to a physical system, it yields a system of lower dimensions, which can accurately describe the dynamics of the original full model. This is, in fact, the great advantage of the POD method and, as a result, the POD technique has been widely utilized in many applications such as modeling turbulence flows [37,3,47,10], shear flows [44,31], channel flows [42,4], etc. and in pattern recognition [32]. However, the use of POD as a reduced-order method for controlling is relatively new. Recently, we used POD technique to simulate and solve an optimal control problems for growing thin films in a horizontal chemical vapor deposition reactor [35] and for the Bénard convection [36]. Also, Kunisch and Volkwein [33] have used POD to control the Burgers equation and Banks et al. [5] have applied POD to design a feedback control for a linear thin shell model.

In this paper, we present a proof-of-concept implementation of the AIM and POD based feedback control for the Kuramoto–Sivashinsky equation(KSE) [8,11]. KSE, which is used to describe long-wave motions of the liquid thin film over a vertical plane, is given by

$$\frac{\partial \eta}{\partial t} + \nu \frac{\partial^4 \eta}{\partial z^4} + \frac{\partial^2 \eta}{\partial z^2} + \eta \frac{\partial \eta}{\partial z} = 0, \tag{1.1}$$

where $z \in [-\pi, \pi]$, $t \geqslant 0$, $\nu > 0$, and are subject to the initial condition

$$\eta(z,0) = \eta_0(z) \tag{1.2}$$

and the boundary conditions

$$\frac{\partial^n \eta}{\partial z^n}(-\pi, t) = \frac{\partial^n \eta}{\partial z^n}(\pi, t), \quad n = 0, 1, 2, 3. \tag{1.3}$$

Eq. (1.1) has also been used to describe the dynamics of laminar flame fronts [41,48,49].

In the next section, we will discuss the numerical algorithms for the solutions employing the AIM and the POD methods. In Section 3, we will focus on the objective of our studies, that is, to control the dynamics of the thin film flow (1.1) using the reduced-order methods. The control techniques that we consider in this paper include both the linear and nonlinear quadratic regulator methods. Numerical results for the linear and nonlinear feedback control employing the AIM and the POD methods will be analyzed and compared in the last section.

2. Reduced-order methods for the KSE

2.1. Reduced-order solution using approximate inertial manifold

The existence and uniqueness of solutions to the KSE (1.1) was first shown by Nicolaenko et al. [43] with the assumption that solutions are odd and periodic. It was also shown that Eq. (1.1) is dissipative and has a finite-dimensional global attractor. That is, its solutions after some transient time can be characterized by a finite set of basis functions. The same results were achieved later for the general periodic case independently in [12,23]. Stability of the KSE (1.1) has been studied extensively over the last decade (see for instance [1,2,16,24–26,43]). The studies of the inertial manifolds for equation (1.1) can be found in [14,17,18,30,45,52]. Also following the work of Foias and Temam [19] one can show that for any initial value:

$$\eta_0 \in \left\{ f \,|\, \eta \text{ is odd, periodic and } \frac{\partial^m f}{\partial z^m} \in L^2(-\pi, \pi) \text{ for } m \geqslant 1 \right\},$$

the solution belongs to a Gevrey class of regularity for all $t > 0$. In particular, $\eta(z,t)$ is analytic in the spatial variable $z \in \mathbb{R}$ for all $t > 0$. In addition, Jolly et al. [27] studied the approximate inertial manifolds for (1.1) both analytically and computationally. Kevrekidis et al. studied (1.1) numerically in [30]. Furthermore, Smyrlis and Papageorgiou [50] computed the Feigenbaum number for the bifurcation cascade of (1.1) as ν varies.

Remark 2.1. If η_0 is odd, the solution $\eta(t)$ remains odd for all t. Also in the derivation of (1.1), $\eta(t)$ is the integral of an odd function. Thus it is natural to restrict our solution to an odd-function space. We denote by $H = \{ f \in L^2_{\text{per}}(-\pi, \pi) | f \text{ is odd} \}$.

Remark 2.2. The operator $A := \partial^4/\partial z^4$ along with boundary conditions (1.3) is a positive definite operator. The domain of A is defined as

$$\mathscr{D}(A) := \left\{ f \in L^2_{\text{odd}}(-\pi, \pi) \,|\, \frac{\partial^n f}{\partial z^n}(-\pi) = \frac{\partial^n f}{\partial z^n}(\pi), \text{ for } n = 0, 1, 2, 3 \right\},$$

so that $A^{-1} : L^2(-\pi,\pi) \to L^2(-\pi,\pi)$ is compact (Rellich's Lemma). Thus there exists a complete orthonormal basis $\{\phi_k(z)\}_{k=1}^{\infty}$ in H, consisting of the eigenfunctions of A. In particular, we have for $k = 1,\ldots,\infty$,

$$\phi_k(z) = \frac{1}{\sqrt{\pi}}\sin(kz) \tag{2.1}$$

with the corresponding eigenvalues

$$\lambda_k = k^4. \tag{2.2}$$

Remark 2.3. We denote by $b(\eta,\xi) = \eta\partial\xi/\partial z$, the bilinear operator for all η and $\xi \in \mathbf{H}^1_{\text{per}}(-\pi,\pi) := \{f \mid f, \frac{\partial f}{\partial z} \in L^2_{\text{per}}(-\pi,\pi)\}$, then Eq. (1.1) can be rewritten in the following differential form

$$\frac{\mathrm{d}\eta}{\mathrm{d}t} + \nu A\eta + A^{1/2}\eta + b(\eta,\eta) = 0, \tag{2.3}$$

for any $\eta \in \mathbf{H}^1_{\text{per}}(-\pi,\pi)$.

Let N be a positive integer, we define a projection

$$P_N : L^2(-\pi,\pi) \to \ \text{Span}\{\phi_k \mid k = 1,\ldots,N\}$$

with

$$Q_N = I - P_N.$$

Then by letting $p = P_N\eta$ and $q = Q_N\eta$, Eq. (2.3) can be split into

$$\frac{\partial p}{\partial t} + \nu A p + A^{1/2} p + P_N b(p+q, p+q) = 0, \tag{2.4}$$

$$\frac{\partial q}{\partial t} + \nu A q + A^{1/2} q + Q_N b(p+q, p+q) = 0, \tag{2.5}$$

where $\eta = p + q$. Eqs. (2.4) and (2.5) refer to the dynamics of the slow and fast manifolds for the solution space, respectively. Due to the existence of inertial manifold for the KSE, the dynamics of q converges quickly to the initial manifold and remains there indefinitely. As a result, for sufficiently large time and sufficiently large N, $\partial q/\partial t$ is negligible and Eq. (2.5) yields (see [27] and references therein)

$$q = -\frac{1}{\nu}A^{-1}(Q_N A^{1/2} q + Q_N b(p+q, p+q)). \tag{2.6}$$

Solution to the infinite-dimensional function q in (2.6) cannot be found explicitly. Instead, it can be approximated by the function $\Phi(p)$, where $\Phi(\cdot)$ solves the exact implicit relation

$$\Phi(p) = -\frac{1}{\nu}A^{-1}(Q_N A^{1/2}\Phi(p) + Q_N b(p + \Phi(p), p + \Phi(p))). \tag{2.7}$$

There are several approaches to approximating the above implicit equation. The simplest one is to assume $\Phi(p) = \Phi_0(p) = 0$ which is known as the linear Galerkin method. Thus the approximated solution is solely p and Eqs. (2.4) and (2.5) become

$$\frac{\partial p}{\partial t} + \nu A p + A^{1/2} p + P_N b(p, p) = 0. \tag{2.8}$$

The first-order nontrivial representation of Φ can be approximated as

$$\Phi_1(p) = -\frac{1}{v}A^{-1}(Q_N A^{1/2}\Phi_0(p) + Q_N b(p + \Phi_0(p), p + \Phi_0(p))) = -\frac{1}{v}A^{-1}Q_N b(p, p). \tag{2.9}$$

Following this approach, one can construct higher-order AIM solution to Eq. (2.7) using the relation of $\Phi_{k+1}(p) = p + \Phi_k(p)$ for any $k \geqslant 0$. Detailed formulations and numerical convergence can be found in [27] and references therein. For our AIM solution to the KSE, we will assume $\eta = p + \Phi_1(p)$ which can be found by solving the differential and algebraic system (2.4) and (2.9). In this case, the approximate solution has the order of convergence of $\sim \lambda_{N+1}^{-\frac{3}{2}}$. The numerical algorithm for computing η is given as follows:

1. Given $p^i = P_N(\eta(t_i))$,
2. Compute $Q_N b(p^i, p^i)$ and $q^i = -(1/v)A^{-1}(Q_N b(p^i, p^i))$,
3. Solve for p^{i+1} from $\partial p/\partial t + vA\,p + A^{1/2}\,p + P_N b(p^i + q^i, p^i + q^i) = 0$,
4. Repeat the process.

The AIM solution corresponding to $v = 0.10$, $N = 10$, and $\eta_0(z) = (5/\sqrt{\pi})\sum_{k=1}^{5}\sin(kz)$ is depicted in Fig. 1. We notice the unstable behavior of $\eta(t)$ as time progresses.

2.2. Reduced-order solution using proper orthogonal decomposition

In this section, we will summarize the process of finding the POD. Detailed description of POD as well as its mathematical properties can be found elsewhere in the literature (see, e.g., [9,35]).

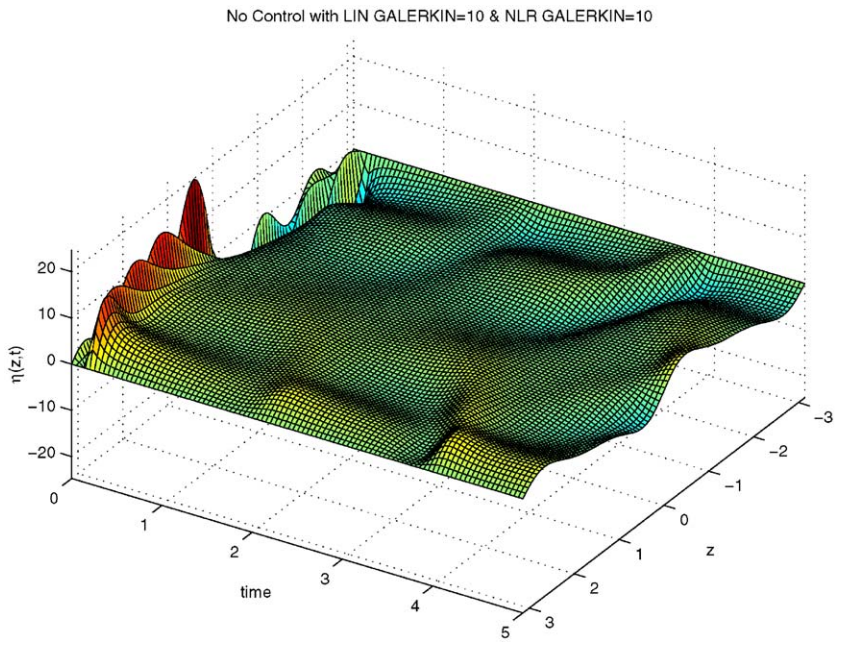

Fig. 1. AIM Solution using 10 linear AIM and 10 Nonlinear AIM Modes ($v = 0.10$).

Let $\{\mathbf{U}_i(z) : 1 \leqslant i \leqslant N_s;\}$ denote the set of N_s observations (also called *snapshots*). In the context of the KSE, these observations could be experimental measurements obtained from sensors or numerical solutions over $[-\pi, \pi]$ taken at different time steps. In our study, we assume that $\{\mathbf{U}_i(z) : 1 \leqslant i \leqslant N_s\}$ is the set of solutions to the KSE at different time steps using the AIM approach. However, in principle, they could be numerical solutions to the KSE using any reliable solver. The POD technique is designed to extract from this set of observations a coherent structure, which has the largest mean square projection on the observations. In other words, we look for a function ϕ^{POD}, or the so-called POD basis element, that most resembles $\{\mathbf{U}_i(z)\}_{i=1}^{N_s}$ in the sense that it maximizes

$$\frac{1}{N_s}\sum_{i=1}^{N_s} |(\mathbf{U}_i, \phi^{\mathrm{POD}})|^2, \tag{2.10}$$

subject to

$$(\phi^{\mathrm{POD}}, \phi^{\mathrm{POD}}) = \|\phi^{\mathrm{POD}}\|^2 = 1,$$

where $(\cdot,\cdot)$ and $\|\cdot\|$ denote the usual $\mathbf{L}^2$ inner product and $\mathbf{L}^2$-norm over $[-\pi, \pi]$, respectively. We choose a special class of trial functions for ϕ^{POD} to be of the form:

$$\phi^{\mathrm{POD}}(z) = \sum_{i=1}^{N_s} a_i \mathbf{U}_i(z), \tag{2.11}$$

where the coefficients a_i are to be determined so that ϕ^{POD} given by expression (2.11) provides a maximum for (2.10). To this end, let us define

$$\mathbf{K}(z, z') := \frac{1}{N_s}\sum_{i=1}^{N_s} \mathbf{U}_i(z)\mathbf{U}_i(z') \text{ and } \mathbf{R}\phi^{\mathrm{POD}} := \int_{-\pi}^{\pi} \mathbf{K}(z, z')\phi^{\mathrm{POD}}(z')\,\mathrm{d}z',$$

where $\mathbf{R} : \mathbf{L}^2([-\pi, \pi]) \to \mathbf{L}^2([-\pi, \pi])$. Then straightforward calculations reveal that

$$(\mathbf{R}\phi^{\mathrm{POD}}, \phi^{\mathrm{POD}}) = \frac{1}{N_s}\sum_{i=1}^{N_s} |(\mathbf{U}_i, \phi^{\mathrm{POD}})|^2.$$

Furthermore, it follows that

$$(\mathbf{R}\phi^{\mathrm{POD}}, \psi) = (\phi^{\mathrm{POD}}, \mathbf{R}\psi) \text{ for any } \phi^{\mathrm{POD}}, \psi \in \mathbf{L}^2([-\pi, \pi]).$$

Thus $\mathbf{R}$ is a nonnegative symmetric operator on $\mathbf{L}^2([-\pi, \pi])$. Consequently, the problem of maximizing expression (2.10) amounts to finding the largest eigenvalue to the eigenvalue problem

$$\mathbf{R}\phi^{\mathrm{POD}} = \lambda\phi^{\mathrm{POD}} \text{ subject to } \|\phi^{\mathrm{POD}}\| = 1 \tag{2.12}$$

or

$$\int_{-\pi}^{\pi} \mathbf{K}(z, z')\phi^{\mathrm{POD}}(z')\,\mathrm{d}z' = \lambda\phi^{\mathrm{POD}} \text{ with } \|\phi^{\mathrm{POD}}\| = 1. \tag{2.13}$$

Substituting expression (2.11) and the definition of $\mathbf{K}$ into Eq. (2.13), we obtain

$$\sum_{i=1}^{N_s}\left[\sum_{k=1}^{N_s}\left(\frac{1}{N_s}\int_{-\pi}^{\pi}\mathbf{U}_i(z')\mathbf{U}_k(z')\,\mathrm{d}z'\right)a_k\right]\mathbf{U}_i(z)=\sum_{i=1}^{N_s}\lambda a_i\mathbf{U}_i(z).$$

This can be rewritten as the eigenvalue problem

$$\mathbf{CV}=\lambda\mathbf{V},$$

where

$$\mathbf{C}_{ik}=\frac{1}{N_s}\int_{-\pi}^{\pi}\mathbf{U}_i(z)\mathbf{U}_k(z)\,\mathrm{d}z \quad \text{and} \quad \mathbf{V}=\begin{bmatrix}a_1\\ a_2\\ \vdots\\ a_{N_s}\end{bmatrix}. \tag{2.14}$$

Since $\mathbf{C}$ is a nonnegative Hermitian matrix, it has a complete set of orthogonal eigenvectors

$$\mathbf{V}^1=\begin{bmatrix}a_1^1\\ a_2^1\\ \vdots\\ a_{N_s}^1\end{bmatrix},\mathbf{V}^2=\begin{bmatrix}a_1^2\\ a_2^2\\ \vdots\\ a_{N_s}^2\end{bmatrix},\ldots,\mathbf{V}^{N_s}=\begin{bmatrix}a_1^{N_s}\\ a_2^{N_s}\\ \vdots\\ a_{N_s}^{N_s}\end{bmatrix}$$

with the corresponding eigenvalues $\lambda_1\geqslant\lambda_2\geqslant\cdots\geqslant\lambda_{N_s}\geqslant 0$. Thus, the solution to the optimization problem for (2.10) is given by

$$\Phi_1^{\mathrm{POD}}=\sum_{i=1}^{N_s}a_i^1\mathbf{U}_i,$$

where a_i^1 are the elements of the eigenvector $\mathbf{V}^1$ corresponding to the largest eigenvalue λ_1. The remaining POD basis elements, Φ_i, $i=2,\ldots,N_s$, are obtained by using the elements of other eigenvectors, $\mathbf{V}^i$, $i=2,\ldots,N_s$.

An alternative approach [35] for finding the solution to maximization of (2.10) is by using the so-called Rayleigh–Ritz method for finding eigenvalues.

The POD basis has certain desirable properties. First, the POD modes can be shown to be orthonormal (see, e.g., [35]). In addition, the POD coefficients are uncorrelated [9]. Finally, POD is the most efficient, in the sense that, for a given number of modes, N, the projection on the subspace used for approximation will contain the most kinetic energy possible in an average sense. More specifically, suppose that we have a solution $v(z,t)$ with $v\in L^2([-\pi,\pi]\times[0,T])$ and an approximation of v^N of v with respect to an *arbitrary* orthonormal basis $\psi_i(z)$,

$$v^N(z,t)=\sum_{i=1}^{N}a_i(t)\psi_i(z),$$

for any arbitrary $N>0$. If the $\psi_i(z)$ have been nondimensionalized, then the coefficients a_i carry the dimension of the quantity v^N. If $v^N(z,t)$ denotes the velocity and $\langle\cdot\rangle$ denotes the time average

operator, then the average kinetic energy per unit mass is given by

$$\left\langle \int_{-\pi}^{\pi} v^N(z,t)v^{N*}(z,t)\,\mathrm{d}z \right\rangle = \left\langle \sum_{i=1}^{N} a_i(t)a_i^*(t) \right\rangle.$$

Consequently, the expression $\langle a_i a_i^* \rangle$ represents the average kinetic energy in the ith-mode. The following lemma establishes the notion of optimality of the POD method.

Lemma 2.4. *Let* $\{\phi_1^{\mathrm{POD}}, \phi_2^{\mathrm{POD}}, \ldots, \phi_N^{\mathrm{POD}}\}$ *denote the orthonormal set of* POD *basis elements and* $(\lambda_1, \lambda_2, \ldots, \lambda_N)$ *denote the corresponding set of eigenvalues. If*

$$v^N(z,t) = \sum_{i=1}^{N} b_i(t)\phi_i^{\mathrm{POD}}(z)$$

denotes the approximation to v *with respect to this basis, then the following hold*:

(a) $\langle b_i(t)b_j^*(t)\rangle = \delta_{ij}\lambda_i$ (*that is, the* POD *coefficients are uncorrelated*).
(b) *For every* N,

$$\sum_{i=1}^{N}\langle b_i(t)b_i^*(t)\rangle = \sum_{i=1}^{N}\lambda_i \geqslant \sum_{i=1}^{N}\langle a_i(t)a_i^*(t)\rangle.$$

The proof of this lemma is straight forward from the optimality of the eigenvalues and can be found in [9].

2.2.1. POD solution

Numerical solutions to the KSE using the POD method described above are obtained using the following procedure:

1. *Generating snapshots*. For the set of observations, we take the AIM solutions shown in Fig. 1 for t dispersing equally from zero to 10 s with the increment of 0.05 s ($N_s = 201$).
2. *Constructing the covariance matrix and its eigenvalues and eigenvectors*. Let $C = (C_{i,j})$, with $C_{i,j} = \frac{1}{201}(\eta(t_i), \eta(t_j))$. Then find the eigenvalues $\{\lambda_i\}_{i=1}^{i=201}$ and the eigenvectors $\{V_i\}_{i=1}^{i=201}$, where $\lambda_1 \geqslant \lambda_2 \geqslant \cdots \geqslant \lambda_{201}$.
3. *Obtaining the POD bases and their energy*. $\phi_i^{\mathrm{POD}}(z) = \sum_{k=1}^{201} V_i^k \eta(z, t_k)$ and $\mathrm{Energy}(M) = \sum_{k=1}^{M}\lambda_k / \sum_{k=1}^{201}\lambda_k$. As mentioned earlier, due to its low viscosity, our uncontrolled solution's behaviors are highly dynamic. The number of POD modes needed to characterize the solutions corresponds directly to the dynamics of the snapshots. In our case, we have $v = 0.10$ and $M = 6$, which corresponds to over 99.99% of energy. For higher viscosity, M is smaller.
4. *Constructing POD solutions*. Assume $\eta^{\mathrm{POD}}(z,t) = \sum_{k=1}^{M}\alpha_k^{\mathrm{POD}}(t)\phi^{\mathrm{POD}}(z)$, where $\alpha_k^{\mathrm{POD}}(t)$ is found through the linear Galerkin formulation.

Numerical solution using the POD method with six POD modes is shown in Fig. 2 and the L^2-norms of the solutions for the POD and AIM techniques, are displayed in Fig. 3. We would like to remark here that the degrees of freedom using the AIM method are already small compared to those using other numerical methods such as the finite element, finite difference, or spectral

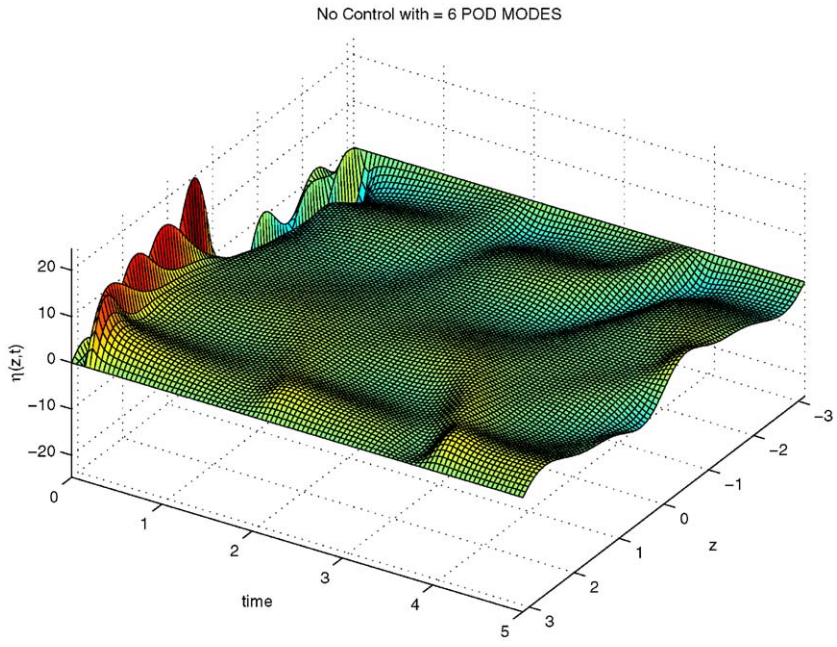

Fig. 2. POD Solution using six POD Modes ($v = 0.10$).

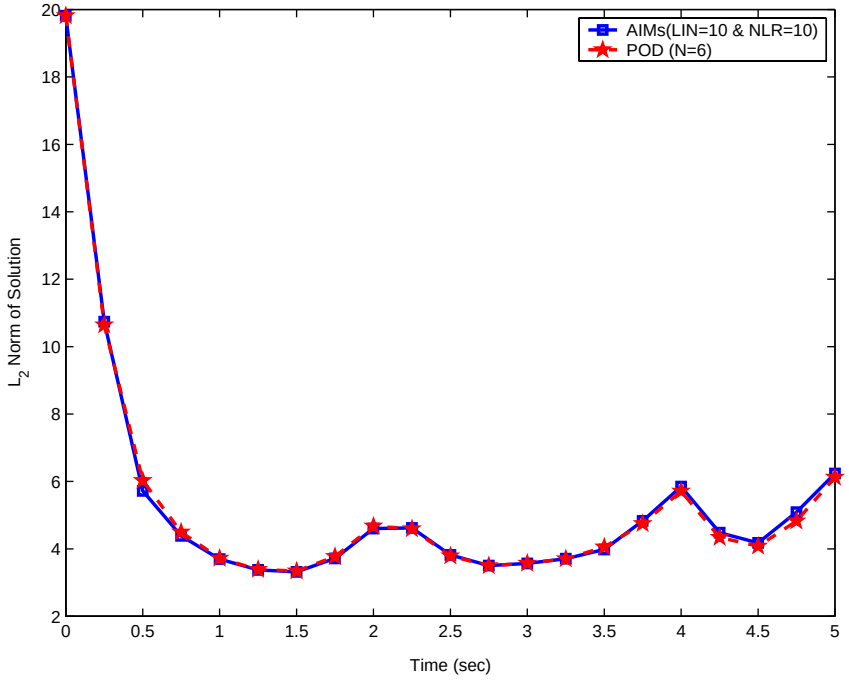

Fig. 3. Relative error between the AIM solution ($N = 10$) and POD solution ($M = 6$) ($v = 0.10$).

methods. The number of modes needed to generate the POD solutions are also remarkably smaller. Such phenomenon is clearly due to the fact that these POD modes are used to describe a more specific set of solutions, namely the snapshots. On the other hand, the 20 AIM modes can be used to represent a larger and more general set of solutions.

3. Feedback control for the reduced-order model

As mentioned earlier, one of the applications of the KSE is to model long-wave motions of the liquid thin film over a vertical plane. Thin liquid films are ubiquitous in industrial and natural processes. A simple and obvious example is the flow of (thin) raindrop down a windowpane under the action of gravity. Another application in the coatings industry is the wet coating of paint that is applied to a vertical wall. The paint will flow downward until the pain has dried; this phenomenon is called "sagging". If the paint layer is of nonuniform thickness, with a thicker region lying above a thin region, a relatively steep front can develop as the paint flows downward. Often this front will develop undulations that lead to growing "fingers" of paint. Such unsightly drip marks in the final dry coating is undesirable for decorative purpose. Nonuniformity in the thickness of downward flowing liquid layers is also a concern in the manufacturing process of photographic films where the film is created as it passes under the falling curtain coated with thin gelatinous fluid containing chemicals such as light sensitive silver halide grains, dye couplers, etc. Therefore, in such applications it is desirable to regulate the film thickness at a desired constant value and as fast as possible (to speed up the process).

For small value of ν, the solution to the Eq. (2.3) becomes oscillatory or unstable (see Fig. 1 or 2 where $\nu = 0.30$). In this section, the optimal control problem that we formulate is to stabilize the film fluctuation by means of blowing or suction at the M_c points $\{z_i\}_{i=1}^{M_c}$ on the wall surface. The actuators are located at $\{z_i\}_{i=1}^{M_c} \in [-\pi, \pi]$ and the proposed controllers are of the form $\delta(z-z_i)*u_i(t)$, where $u_i(t)$ is the control input and $\delta(z-z_i)$ is the *Dirac* delta function at z_i. That is, the control system is described by

$$\frac{\partial \eta}{\partial t} + \nu \frac{\partial^4 \eta}{\partial z^4} + \frac{\partial^2 \eta}{\partial z^2} + \eta \frac{\partial \eta}{\partial z} = F_c(z,t), \tag{3.1}$$

where

$$F_c(z,t) = \sum_{i=1}^{M_c} u_i(t)\delta(z-z_i). \tag{3.2}$$

3.1. Linear and nonlinear feedback controllers

Let

$$\eta^N(z,t) = \sum_{i=1}^{N} \alpha_i(t)\phi_i(z)$$

be the approximating solution to the KSE, where $\{\phi_i(z)\}_{i=1}^N$ are either the Galerkin AIM or POD bases. Then from the weak form of Eq. (3.1), we obtain

$$\dot{\vec{w}}(t) = \mathscr{A}\vec{w} + \vec{\mathbf{N}}(\vec{w}) + B\vec{\mathbf{u}}, \tag{3.3}$$

where

$$\vec{w} = \begin{bmatrix} \alpha_1(t) \\ \vdots \\ \alpha_N(t) \end{bmatrix}, \quad \mathscr{A} = (\mathscr{A}_{ij}), \quad \text{with } \mathscr{A}_{ij} = \int_{-\pi}^{\pi} \left(\nu \frac{\partial^4 \phi_i}{\partial z^4} + \frac{\partial^2 \phi_i}{\partial z^2} \right) \phi_j \, \mathrm{d}z, \tag{3.4}$$

$$\vec{\mathbf{N}}(\vec{w}) = \begin{bmatrix} \mathscr{N}_1(t) \\ \vdots \\ \mathscr{N}_N(t) \end{bmatrix} \text{ with } \mathscr{N}_j(t) = \sum_{i=1}^{N} \sum_{k=1}^{N} \alpha_i(t)\alpha_k(t) \int_{-\pi}^{\pi} \phi_i \frac{\partial \phi_k}{\partial z} \phi_j \, \mathrm{d}z, \tag{3.5}$$

$$B = \begin{bmatrix} \phi_1(z_1) & \cdots & \phi_1(z_{M_c}) \\ \vdots & & \vdots \\ \phi_N(z_1) & \cdots & \phi_N(z_{M_c}) \end{bmatrix}, \quad \vec{\mathbf{u}} = \begin{bmatrix} u_1(t) \\ \vdots \\ u_N(t). \end{bmatrix} \tag{3.6}$$

Associated with the finite dimensional system (3.3) is the quadratic cost functional

$$\begin{aligned} J(\vec{\mathbf{u}}) &= \int_0^\infty \left[c_0 \|\eta(t)\|^2_{L^2(-\pi,\pi)} + \sum_{j=1}^{M_c} c_j \|u_j(t)\|^2 \right] \mathrm{d}t \\ &= \int_0^\infty \left[c_0 \sum_{i=1}^{N} \alpha_i(t)^2 + \sum_{j=1}^{M_c} c_j \|u_j(t)\|^2 \right] \mathrm{d}t \\ &= \int_0^\infty \left[\vec{w}^{\mathrm{T}} Q \vec{w} + \vec{\mathbf{u}}^{\mathrm{T}} R \vec{\mathbf{u}} \right] \mathrm{d}t, \end{aligned} \tag{3.7}$$

where $c_k > 0$ for $k = 0, 1, \ldots, M_c$ are design parameters with $Q = c_0 I_N$ and $R = \mathrm{diag}\{c_1, \ldots, c_{M_c}\}$. The optimal control problem is to find a state feedback control $\vec{\mathbf{u}}^*(\vec{w})$ which minimizes the cost for all possible initial conditions.

3.1.1. A linear feedback control

Assuming the nonlinear term $\vec{\mathbf{N}}(\vec{w})$ in Eq. (3.3) is small, a suboptimal feedback control $\vec{\mathbf{u}}^*$ can be obtained by using the well-known linear quadratic regulator theory. That is,

$$\vec{\mathbf{u}}^*(\vec{w}) = -\tfrac{1}{2} R^{-1} B^{\mathrm{T}} \Pi \vec{w}, \tag{3.8}$$

where Π is positive definite and symmetric matrix solution of the *algebraic Riccati equation*:

$$\Pi\mathscr{A} + \mathscr{A}^{\mathrm{T}}\Pi - \Pi B R^{-1} B^{\mathrm{T}c} \Pi + Q = 0. \tag{3.9}$$

The theories for this linear quadratic regulator (LQR) problem have been well established for both the finite and infinite-dimensional problems (see, e.g., [6,34]). In addition, stable and robust algorithms for solving the Riccati equation have already been developed and are well documented in many places in the literature and in textbooks.

3.1.2. A nonlinear feedback control

For the nonlinear case, the optimal feedback control is known to be of the form

$$u^*(t) = -\tfrac{1}{2}R^{-1}B^{\mathrm{T}}V_{\vec{w}}(\vec{w}),$$

where the function V is the solution to the Hamilton–Jacobi–Bellman (HJB) equation

$$V_{\vec{w}}^{\mathrm{T}}(\vec{w})(\mathscr{A}\vec{w} + \vec{\mathbf{N}}) - \tfrac{1}{4}V_{\vec{w}}^{\mathrm{T}}(\vec{w})BR^{-1}B^{\mathrm{T}}V_{\vec{w}}(\vec{w}) + \vec{w}^{\mathrm{T}}Q\vec{w} = 0. \tag{3.10}$$

The HJB equation itself is very difficult to solve analytically for any but the simplest problems, however. Thus efforts have been made to numerically approximate the solution of the HJB equation, or to solve a related problem producing a suboptimal control, or to use some other process in order to obtain a usable feedback control. For a comprehensive comparison study of nonlinear feedback control methodologies we refer the interested reader to [7]. In the case where the nonlinear term $\vec{\mathbf{N}}(\vec{w})$ is not too complex, for example, when it contains only one level of nonlinearity like the quadratic term in the KSE, the power series approximation method as proposed by Garrard and others (see, e.g., [22]) has been shown to be very effective [7]. In addition, it has the advantages that it is very easy to implement and requires less computational time as some other methods do.

In the power series method to approximate $V(\vec{w})$, we consider the representation $V(\vec{w}) = \sum_{n=0}^{\infty} | V_n(\vec{w})$, where each $V_n(\vec{w}) = \mathrm{O}(\vec{w}^{n+2})$. Substituting the expansion into the HJB equation results in

$$\left(\sum_{n=0}^{\infty}(V_n)_{\vec{w}}^{\mathrm{T}}\right)\left(\mathscr{A}\vec{w} + \vec{\mathbf{N}}(\vec{w})\right) - \frac{1}{4}\left(\sum_{n=0}^{\infty}(V_n)_{\vec{w}}^{\mathrm{T}}\right)BR^{-1}B^{\mathrm{T}}\left(\sum_{n=0}^{\infty}(V_n)_{\vec{w}}\right) + \vec{w}^{\mathrm{T}}Q\vec{w} = 0.$$

By separating out the powers of $\vec{w}$ we obtain the following equations:

$$(V_0)_{\vec{w}}^{\mathrm{T}}\mathscr{A}\vec{w} - \tfrac{1}{4}(V_0)_{\vec{w}}^{\mathrm{T}}BR^{-1}B^{\mathrm{T}}(V_0)_{\vec{w}} + \vec{w}^{\mathrm{T}}Q\vec{w} = 0, \tag{3.11}$$

$$(V_1)_{\vec{w}}^{\mathrm{T}}\mathscr{A}\vec{w} - \tfrac{1}{4}(V_1)_{\vec{w}}^{\mathrm{T}}BR^{-1}B^{\mathrm{T}}(V_0)_{\vec{w}} - \tfrac{1}{4}(V_0)_{\vec{w}}^{\mathrm{T}}BR^{-1}B^{\mathrm{T}}(V_1)_{\vec{w}} + (V_0)_{\vec{w}}^{\mathrm{T}}\vec{\mathbf{N}}(\vec{w}) = 0, \tag{3.12}$$

$$(V_n)_{\vec{w}}^{\mathrm{T}}\mathscr{A}\vec{w} - \frac{1}{4}\sum_{k=0}^{n}[(V_k)_{\vec{w}}^{\mathrm{T}}BR^{-1}B^{\mathrm{T}}(V_{n-k})_{\vec{w}}] + (V_{n-1})_{\vec{w}}^{\mathrm{T}}\vec{\mathbf{N}}(\vec{w}) = 0, \tag{3.13}$$

where $n = 2, 3, 4, \ldots$.

Eq. (3.11) can be solved with $V_0(\vec{w}) = \vec{w}^{\mathrm{T}}\Pi\vec{w}$, where the symmetric positive definite matrix Π solves the Riccati equation (3.9). This gives the standard linear control. Eqs. (3.12) and (3.13) can be solved for V_n, $n = 1, 2, 3, \ldots$, by following the method proposed by Garrard [22]. Using the

substitution $(V_0)_{\vec{w}} = 2\Pi\vec{w}$ in Eq. (3.12) we obtain

$$(V_1)_{\vec{w}}^{\mathrm{T}}\mathscr{A}\vec{w} - \tfrac{1}{4}(V_1)_{\vec{w}}^{\mathrm{T}}BR^{-1}B^{\mathrm{T}}(2\Pi\vec{w}) - \tfrac{1}{4}(2\vec{w}^{\mathrm{T}}\Pi)BR^{-1}B^{\mathrm{T}}(V_1)_{\vec{w}} + (2\vec{w}^{\mathrm{T}}\Pi)\vec{\mathbf{N}}(\vec{w}) = 0.$$

Rearranging some terms, we find

$$\vec{w}^{\mathrm{T}}[\mathscr{A}^{\mathrm{T}}(V_1)_{\vec{w}} - \Pi BR^{-1}B^{\mathrm{T}}(V_1)_{\vec{w}} + 2\Pi\vec{\mathbf{N}}(\vec{w})] = 0.$$

The quantity inside the brackets is zero when $(V_1)_{\vec{w}} = -2(\mathscr{A}^{\mathrm{T}} - \Pi BR^{-1}B^{\mathrm{T}})^{-1}\Pi\vec{\mathbf{N}}(\vec{w})$. This along with the $(V_0)_{\vec{w}}$ term gives a quadratic feedback control law of the form

$$u^*(t) = -R^{-1}B^{\mathrm{T}}[\Pi\vec{w} - (\mathscr{A}^{\mathrm{T}} - \Pi BR^{-1}B^{\mathrm{T}})^{-1}\Pi\vec{\mathbf{N}}(\vec{w})]. \tag{3.14}$$

3.2. Numerical results and comparisons

Consider $v = 0.10$ and the initial condition

$$\eta_0(z) = \frac{5}{\sqrt{\pi}}\sum_{k=1}^{5}\sin(kz),$$

solutions to the uncontrolled problem using the reduced-order AIM and POD methods are depicted in Figs. 1 and 2, respectively. Fig. 3 shows that the L^2-norm of $\eta(t)$, which represents fluctuations of the film thickness, becomes volatile after 5 s. To control the fluctuations (i.e., to regulate the film thickness), we place two controllers at $z = \pi/3$ and $2\pi/3$. We would like to remark here that at least two controllers are needed due to the highly dynamic behavior of the fluctuations. For other cases when the viscosity v is larger, the number of required controllers may be less. Linear feedback controllers using Eq. (3.8) for the AIM and the POD reduced-order systems are obtained and applied. The time evolutions of linear feedback control solutions for the AIM and POD systems are shown on the top and bottom of Fig. 4, respectively. Stabilization was achieved and the fluctuations diminishes after 2.5 s. We also note that the locations of the actuators are not necessarily optimal (i.e., other locations could yield more control authority). Fig. 5 depicts the numerical solutions of the nonlinear feedback control law (3.14). The fluctuations of the reduced-order AIM and POD systems are driven down to zero. Performances of the linear and nonlinear are not transparent from Figs. 4 and 5. To see the effectiveness of the nonlinear controllers, we show in Fig. 6 the L^2-norms of the uncontrolled, linearly controlled as well as the nonlinearly controlled solutions. It is evident that the controlled solutions using the nonlinear quadratic feedback control law (3.14) decay to zero more quickly. Achieving stabilization at a faster rate is vital in the manufacturing process because it increases production rate (higher throughput) and thus increases profitability. In addition, real-time model-based control of manufacturing processes requires numerical integration of the continuous mathematical model at each discrete-time step at which the real-time processor runs. Although both AIM and POD based reduced-order systems achieve the same control performance, POD based system achieves it using only five POD modes (compared to 40–20 each for the slow and fast manifolds respectively –which is the size of the manifold for AIM). Since the size of the POD finite dimensional system is smaller, it is more applicable for real-time model-based feedback control implementation.

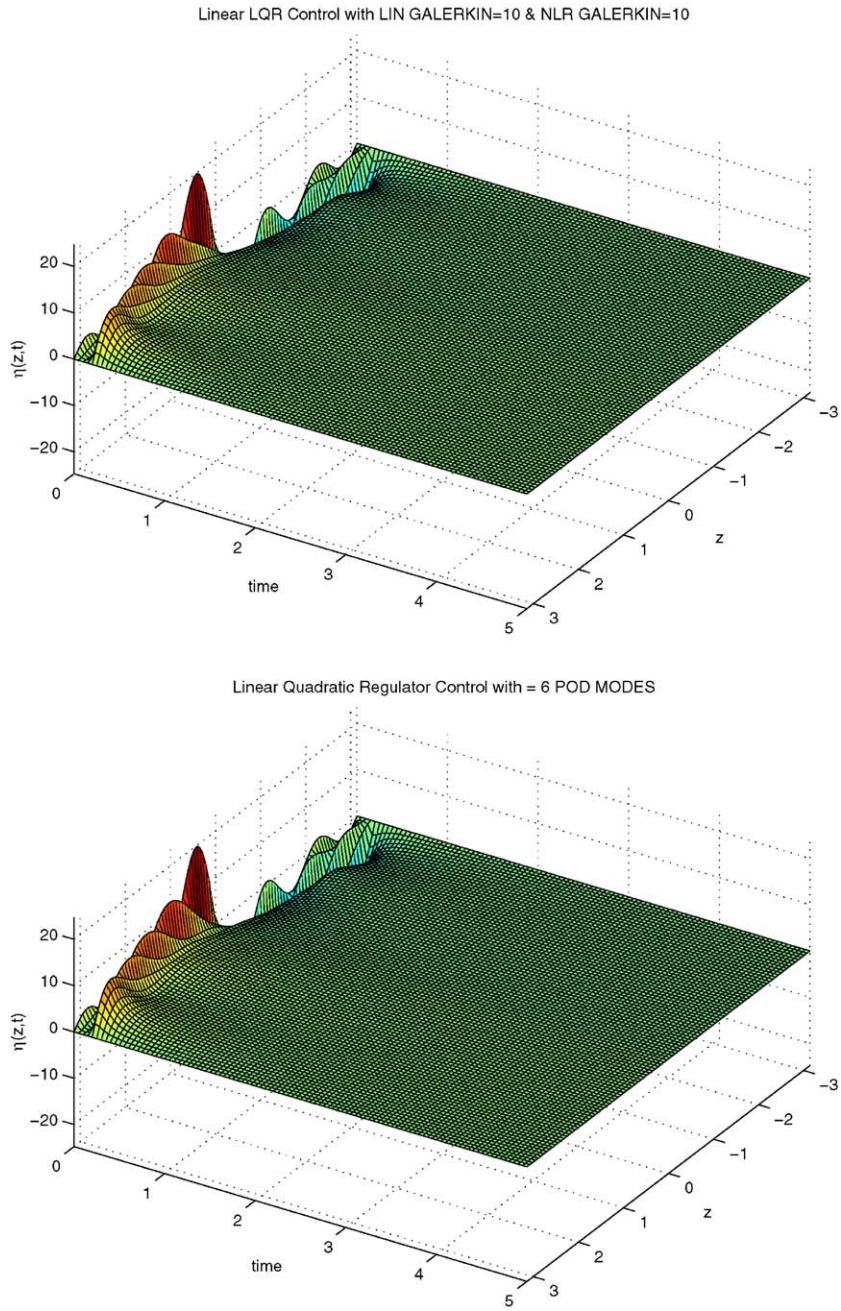

Fig. 4. Reduced-order feedback control solutions using linear quadratic regulator on AIM (top) and on POD (bottom) ($v = 0.10$).

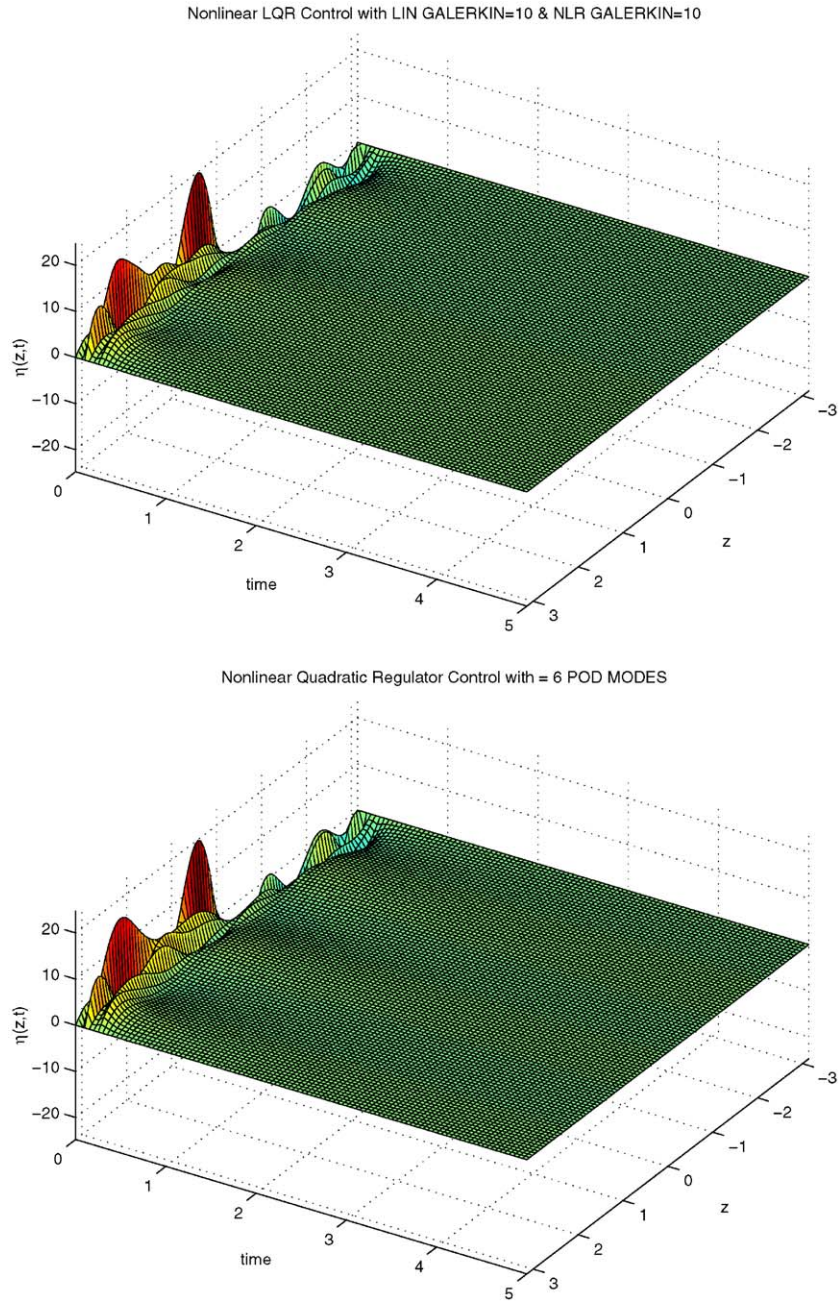

Fig. 5. Reduced-order feedback control solutions using nonlinear quadratic regulator on AIM (top) and on POD (bottom) ($v = 0.10$).

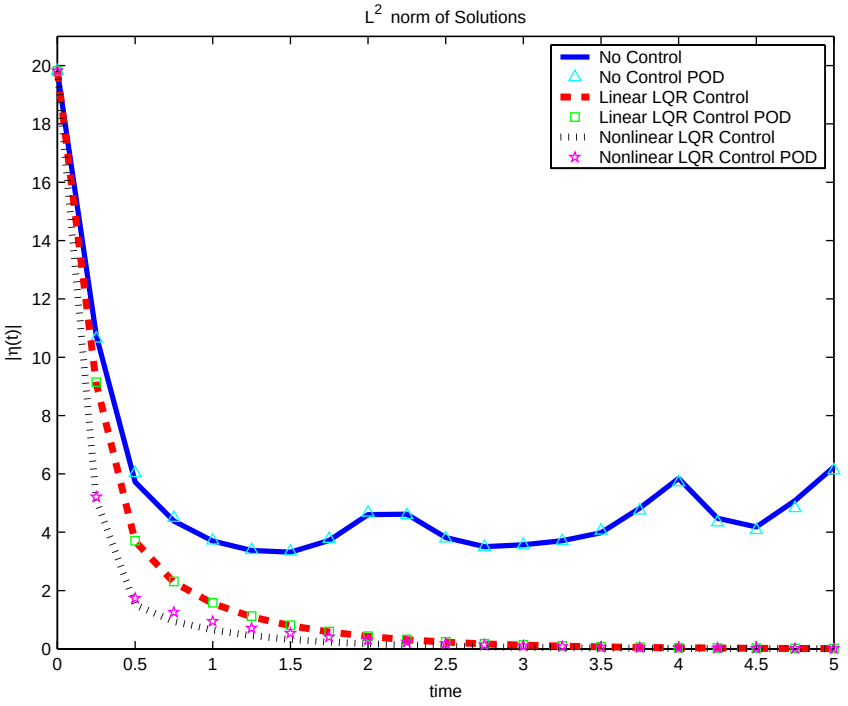

Fig. 6. L^2-norms for the solutions of the controlled and uncontrolled problem using Reduced-order AIM and POD with linear and nonlinear quadratic regulator feedback controls ($\nu = 0.10$).

4. Summary

We have successfully implemented reduced-order-based modeling and feedback control for the long wave perturbations for the viscous film flows, particularly, the KSE. The associated difficulties are due to infinite dimensionality and the nonlinearity, which resembles the convection of many fluid applications, such as the Navier–Stokes equations. We discussed two reduced-order methods, the AIM and the POD. We have shown that both methods can convert an infinite-dimensional nonlinear system to that of smaller dimensions, which optimal feedback controls can be designed and efficiently synthesized. For the feedback control methodologies, we apply the linear and nonlinear quadratic regulators, which are the first- and second-order approximated solutions of the HJB equation, respectively. Numerical solutions of the controlled problem are presented and the results show the improved performance of the nonlinear feedback control over the linear one.

Acknowledgements

The authors would like to thank Professor H. Thomas Banks at North Carolina State University, Professor Yannis G. Kevrekidis at Princeton University and Professor Edriss E. Titi at the University of California, Irvine for the stimulating and fruitful discussions. The authors also would like to thank

the Special Research Center on Optimization and Control at Karl Franzens Universität Graz for their kind hospitality during the *Workshop on the Proper Orthogonal Decomposition and its Applications*, when part of this work was completed. This research was partially supported by the DOD-MURI grant F49620-95-1-0447 through the Center for Intelligent Design and Manufacturing in Electronics and Materials and by the California State University Program for Research, Scholarship and Creative Activity Grants at Fullerton.

References

[1] C.M. Alfaro, M.C. Depassier, A five-mode bifurcation analysis of a Kuramoto–Sivashinsky equation with dispersion, Phys. Lett. A 184 (1994) 184–189.
[2] D. Armbruster, J. Guckenheimer, P. Holmes, Kuramoto–Sivashinsky dynamics on the center-unstable manifold, SIAM J. Appl. Math. 49 (1989) 676–691.
[3] N. Aubry, P. Holmes, J.L. Lumley, E. Stone, The dynamics of coherent structures in the wall region of a turbulent boundary layer, J. Fluid Mech. 192 (1988) 115–173.
[4] K.S. Ball, L. Sirovich, L.R. Keefe, Dynamical eigenfunction decomposition of turbulent channel flow, Internat. J. Numer. Methods Fluids 12 (1991) 585–604.
[5] H.T. Banks, R.C.H. Del Rosario, R.C. Smith, Reduced order model feedback control design: numerical implementation in a thin shell model, Center for Research in Scientific Computation, North Carolina State University, Technical Report CRSC-TR98-27, 1998; IEEE Trans. AC, submitted for publication.
[6] H.T. Banks, R.C. Smith, Y. Wang, Smart Material Structures: Modeling, Estimation, and Control, Masson/Wiley, Paris/Chichester, 1996.
[7] S.C. Beeler, H.T. Tran, H.T. Banks, Feedback control methodologies for nonlinear systems, J. Optim. Theory Appl. 107 (1) (2000) 1–33.
[8] D.J. Benney, Long waves in liquid films, J. Math. Phys. 45 (1966) 150–155.
[9] G. Berkooz, Oberservations on the proper orthogonal decomposition, in: T.B. Gatski, et al., (Eds.), Studies in Turbulence, Springer, New York, 1992, pp. 229–247.
[10] G. Berkooz, P. Holmes, J.L. Lumley, J.C. Mattingly, Low-dimensional models of coherent structures in turbulence, Phys. Rep. 287 (1997) N4:338–384.
[11] H.C. Chang, Wave evolution on a falling film, Ann. Rev. Fluid Mech. 26 (1994) 103–136.
[12] P. Collet, J.-P.Eckmann, H. Epstein, J. Stubbe, A global attracting set for the Kuramoto–Sivashinsky equation, Comm. Math. Phys. 152 (1993) 203–214.
[13] P. Constantin, C. Foias, Navier–Stokes Equations, University of Chicago Press, Chicago, 1982.
[14] P. Constantin, C. Foias, B. Nicolaenko, R. Temam, Spectral barriers and inertial manifolds for dissipative partial differential equations, J. Dyn. Differential Equations 1 (1989) 45–73.
[15] A. Debussche, R. Temam, Inertial manifolds and their dimensions, in: S.I. Andersson, et al., (Eds.), Dynamical Systems: Theory and Applications, World Scientific, Singapore, 1993.
[16] C. Foias, I. Kukavica, Determining nodes for the Kuramoto–Sivashinsky equation, preprint, 1994.
[17] C. Foias, B. Nicolaenko, G.R. Sell, R. Temam, Inertial manifolds for the Kuramoto–Sivashinsky equation and an estimate of their lowest dimension, J. Math. Pures Appl. 67 (1988) 197–226.
[18] C. Foias, G.R. Sell, R. Temam, Inertial manifolds for nonlinear evolutionary equations, J. Differential Equations 73 (1988) 309–353.
[19] C. Foias, R. Temam, Gevrey class regularity for the solutions of the Navier–Stokes equations, J. Funct. Anal. 87 (1989) 359–369.
[20] C. Foias, E.S. Titi, Determining nodes, finite difference schemes and inertial manifolds, Nonlinearity 4 (1991) 135–153.
[21] B. Garca-Archilla, J. Novo, E.S. Titi, Postprocessing the Galerkin method: a novel approach to approximate inertial manifolds, SIAM J. Math. Anal. 35 (N3) (1998) 941–972.
[22] W.L. Garrard, D.F. Enns, S.A. Snell, Nonlinear feedback control of highly manoeuvrable aircraft, Internat. J. Control 56 (1992) N4:799–812.

[23] J. Goodman, Stability of the Kuramoto–Sivashinsky and related systems, Comm. Pure Appl. Math. 47 (1994) 293–306.
[24] J.M. Hyman, B. Nicolaenko, The Kuramoto–Sivashinsky equation: a bridge between PDEs and dynamical systems, Physica D 18 (1986) 113–126.
[25] J.M. Hyman, B. Nicolaenko, Order and complexity in the Kuramoto–Sivashinsky model of weakly turbulent interfaces, Physica D 23 (1986) 265–292.
[26] J.S. Il'yashenko, Global analysis of the phase portrait for the Kuramoto–Sivashinsky equation, J. Dyn. Differential Equations 4 (1992) 585–615.
[27] M.S. Jolly, I.G. Kevrekidis, E.S. Titi, Approximate inertial manifolds for the Kuramoto–Sivashinsky equation: analysis and computations, Physica D 44 (1990) 38–60.
[28] D.A. Jones, E.S. Titi, A remark on quasi-stationary approximate inertial manifolds for the Navier–Stokes equations, SIAM J. Math. Anal. 25 (N3) (1994) 894–914.
[29] D.A. Jones, E.S. Titi, C^1 approximations of inertial manifolds for dissipative nonlinear equations, J. Differential Equations 127 (N1) (1996) 54–86.
[30] I.G. Kevrekidis, B. Nicolaenko, J.C. Scovel, Back in the saddle again: a computer assisted study of the Kuramoto–Sivashinsky equation, SIAM J. Appl. Math. 50 (1990) 760–790.
[31] M. Kirby, J.P. Boris, L. Sirovich, A proper orthogonal decomposition of a simulated supersonic shear layer, Internat. J. Numer. Methods Fluids 10 (1990) 411–428.
[32] M. Kirby, L. Sirovich, Application of the Karhunen–Loève procedure for the characterization of human faces, IEEE Trans. Pattern Anal. Mach. Intell. 12 (1990) N1:103–108.
[33] K. Kunisch, S. Volkwein, Control of the Burgers equation by a reduced-order approach using proper orthogonal decomposition, J. Optim. Theory Appl. 102 (2) (1999) 345–371.
[34] I. Lasiecka, R. Triggiani, Differential and Algebraic Riccati Equations with Application toBoundary/Point Control Problems, Springer, New York, 1991.
[35] H.V. Ly, H.T. Tran, Proper orthogonal decomposition for flow calculations and optimal control in a horizontal CVD reactor, Quart. Appl. Math. 60 (4) (2002) 631–656.
[36] H.V. Ly, H.T. Tran, Modeling and control of physical processes using proper orthogonal decomposition, Comput. Math. Appl. 33 (2001) 223–236.
[37] J.L. Lumley, The structure of inhomogeneous turbulent flows, in: A.M. Yaglom, V.I. Tatarski (Eds.), Atmospheric Turbulence and Radio Wave Propagation, Nauka, Naurka, 1967, pp. 166–178.
[38] L.G. Margolin, D.A. Jones, An approximate inertial manifold for computing Burgers' equation. Experimental mathematics: computational issues in nonlinear science, Physica D 60 (N1-4) (1992) 175–184.
[39] M. Marion, Approximate inertial manifolds for the pattern formation Cahn-Hilliard equations, Math. Model Numer. Anal. 23 (1989) 463–488.
[40] M. Marion, Approximate inertial manifolds for the reaction diffusion equations in high space dimension, J. Dyn. Differential Equations 1 (1989) 245–267.
[41] D.M. Michelson, G.I. Sivashinsky, Nonlinear analysis of hydrodynamics instability in laminar flames II. Numerical experiments, Acta Astronaut. 4 (1977) 1207–1221.
[42] P. Moin, R.D. Moser, Characteristic-eddy decomposition of turbulence in a channel, J. Fluids Mech. 200 (1989) 417–509.
[43] B. Nicolaenko, B. Scheurer, R. Temam, Some global dynamical properties of the Kuramoto–Sivashinsky equation: nonlinear stability and attractors, Physica D 16 (1985) 155–183.
[44] M. Rajaee, S.K.F. Karlson, L. Sirovich, Low-dimensional description of free-shear-flow coherent structures and their dynamical behavior, J. Fluid Mech. 258 (1994) 1–29.
[45] J.C. Robinson, Inertial manifolds for the Kuramoto–Sivashinsky equation, Phys. Lett. A 184 (1994) 190–193.
[46] G.R. Sell, Y.C. You, Inertial manifolds—the nonself-adjoint case, J. Differential Equations 96 (1992) 203–255.
[47] L. Sirovich, Turbulence and the dynamics of coherent structures, part II: symmetries and transformations, Quart. Appl. Math. XLV (1987) N3:573–582.
[48] G.I. Sivashinsky, Nonlinear analysis of hydrodynamics instability in laminar flames I. Derivations of basic equations, Acta Astronaut. 4 (1977) 1177–1206.
[49] G.I. Sivashinsky, On flame propagation under conditions of stoichiometry, SIAM J. Appl. Math. 39 (1980) 67–82.

[50] Y.S. Smyrlis, D.T. Papageorgiou, Predicting chaos for infinite dimensional dynamical systems: the Kuramoto–Sivashinsky equation, a case study, Proc. Natl. Acad. Sci. USA 88 (1991) 11129–11132.
[51] R. Temam, Infinite-Dimensional Dynamical Systems in Mechanics and Physics, Applied Mathematical Sciences, Vol. 68, Springer, New York, 1988.
[52] R. Temam, X. Wang, Estimates on the lowest dimension of inertial manifolds for the Kuramoto–Sivashinsky equation in the general case, Differential Integral Equations 7 (1994) 1095–1108.
[53] E.S. Titi, On approximate inertial manifolds to the Navier–Stokes equations, J. Math. Anal. Appl. 149 (1990) 540–557.